

THE UNIVERSITY OF MICHIGAN
COLLEGE OF ENGINEERING
Department of Nuclear Engineering

Technical Report

SOLUTION OF THE TWO-GROUP NEUTRON TRANSPORT EQUATION

PART II

D. R. Metcalf
P. F. Zweifel

ORA Project 01046

supported by:

NATIONAL SCIENCE FOUNDATION
GRANT NO. GK-1713
WASHINGTON, D.C.

administered through:

OFFICE OF RESEARCH ADMINISTRATION ANN ARBOR

January 1968

SOLUTION OF THE TWO-GROUP NEUTRON TRANSPORT EQUATION
PART II*

D. R. Metcalf[†] and P. F. Zweifel
Department of Nuclear Engineering
The University of Michigan
Ann Arbor, Michigan

Number of Pages: 31
Number of Tables: 5
Number of Figures: 7

*Based in part on a Ph.D. thesis at The University of Michigan. Work supported in part by National Science Foundation.

[†]Atomic Energy Commission Predoctoral Fellow (1964-67). Present address, Department of Nuclear Engineering, University of Virginia, Charlottesville, Virginia.

Proposed Running Head: Two-Group Neutron Transport--II

Mail Proofs to: Professor Dale R. Metcalf
Department of Nuclear Engineering
School of Engineering and Applied Science
University of Virginia
Charlottesville, Virginia 22901

ABSTRACT

Particular numerical methods are described for solving the two-group neutron transport equations obtained in a companion paper. Numerical solutions are presented for the Milne problem and the constant source problem, and the results are compared with P_1 , P_3 , and double P_1 calculations. The most interesting result is the occurrence of a resonance in the continuum expansion coefficient which appears to be due to a zero of the dispersion function $\Omega(z)$ in the unphysical Riemann sheet.

I. INTRODUCTION

In a previous paper, hereafter denoted by I,¹ the general two-group, half-range eigenfunction expansion such as is appropriate to the study of neutron transport in half-spaces was reduced to a form convenient for numerical analysis. The application was then made to two typical half-space problems; the Milne and constant isotropic source problems. The shape of the arbitrary two-component function which is expanded was determined by the application of appropriate boundary conditions. The judicious use of typical X-function identities in the general case and for the applications provided some important simplifications to the final equations. The result for any typical half-space problem was a pair of coupled equations for two unknowns, a discrete and a continuum mode expansion coefficient, Eqs. (I-58a) and (I-58b). With these two expansion coefficients assumed as known, one additional equation [Eq. (I-58c)] provided directly the solution for the remaining expansion coefficient. The angular fluxes and the total fluxes and currents are then expressed in terms of these expansion coefficients and the normal modes of the two-group transport equation.

In this paper the necessary numerical procedures for an exact, complete solution to typical two-group, half-space problems is presented. The logical steps in the numerical procedure are as follows:

1. The discrete eigenvalues (roots) of the dispersion equation are found [Eq. (I-10)].
2. By an iteration procedure using Gauss quadrature, a nonlinear singular integral equation is solved for an unknown function denoted by $\kappa(-z)$ which is

directly related to the X-function and $\gamma(\mu)$. [The X-function is introduced in Eq. (I-33); $\gamma(\mu)$ is defined in (I-35).]

3. The set of coupled equations [Eqs. (I-58)], is then solved for the expansion coefficients by an iteration procedure.

4. With the expansion coefficients known the two-group angular fluxes, as well as total fluxes and currents, are easily calculated.

The spherical harmonic solutions to the two-group neutron transport equation in the P_1 , P_3 , and DP_1 approximations are briefly discussed in Section IV. These solutions are developed in order to compare with the exact results and thus derive a feeling for the validity of the various approximation methods. Finally in Section V numerical results are presented for a set of light water problems. We refer the reader to I for notation and appropriate equations.

The most interesting result is the occurrence of resonance in the continuum expansion coefficient (see Figs. 1 and 2). These "quasi-discrete modes" are already known in certain thermalization problems, and have been attributed to discrete eigenvalues lying in the unphysical Riemann sheet (for review and further references, cf. Ref. 3 of Part I). There is no question in our minds that such an explanation is correct in the present case as well for the following reasons. We note¹ that for certain values of the parameters, the two-group dispersion function has one pair of zeros while for other values two pairs occur. It seems likely that two pairs of zeros always occur, but in certain cases one pair disappears through the cut onto the unphysical sheet.

Since, at least in the one-speed case, the continuum expansion coefficient varies as $^4 [\Omega^+(\nu)\Omega^-(\nu)]^{-1}$, if this pole on the unphysical sheet lies sufficiently close to the cut a resonance behavior is exactly what one would expect. This question is being studied further at the present time.

II. DISCRETE EIGENVALUES AND COMPUTATION OF $\gamma(\mu)$

For the problems studied in this paper, the discrete eigenvalues satisfy the conditions

$$|\eta_i| > 1,$$

and

$$\Omega(\eta_i) = \Omega(-\eta_i) = 0.$$

Also from Table 1¹ the discrete eigenvalues of interest here are two in number and are real for each case studied.

The "regula falsi" method² for finding the roots of a transcendental equation is used to solve the dispersion equation [Eq. (I-10)]. In practice

$\Omega(z)$ is calculated for z near unity and then z is advanced in small positive values until $\Omega(z)$ changes sign. By linear inverse interpolation the root is then calculated to any desired accuracy. With the discrete eigenvalues known, we proceed to the calculation of $\gamma(\mu)$.

The method of Shure and Natelson³ is used to obtain a nonlinear singular integral equation for a function $\kappa(-\mu)$ which is directly related to the X-function and $\gamma(\mu)$. For this analysis the two-group X-function identities that we need are

$$X(z) = \int_0^1 \frac{\gamma(\mu)f(\mu)d\mu}{\mu-z} \quad (1a)$$

and

$$X(z)X(-z) = \frac{\Omega(z)}{\Omega(\infty)(\eta_1^2 - z^2)} \quad (1b)$$

where

$$f(\mu) = \frac{\Omega^+(\mu) - \Omega^-(\mu)}{2\pi i \mu} = C_{22} + [C_{11} - 2C_{\mu\tau}(\mu) - 2C_{\mu\tau}(\sigma\mu)]\theta_1(\mu) - 2C_{\mu\tau}(1/\sigma\mu)\theta_2(\mu) \quad (2)$$

and the dispersion relation yields

$$\Omega(\infty) = 1 - \frac{2C_{11}}{\sigma} - 2C_{22} + \frac{4C}{\sigma} .$$

The proof of these identities parallels closely that for the one-group case.⁴

We define a function $\kappa(z)$,

$$\kappa(z) = \left(\frac{1}{X(0)} - z \right) X(z) \quad (3)$$

with the property

$$\kappa(0) = \kappa(\infty) = 1$$

where $X(0)$ is given by

$$X(0) = \left[\frac{1}{\Omega(\infty)\eta_1^2} \right]^{1/2} .$$

By solving Eq. (3) for $X(z)$ and substituting into Eq. (1b), we obtain

$$\frac{\Omega(z)}{\kappa(z)\kappa(-z)} = \frac{1 - \frac{z^2}{\eta_1^2}}{1 - z^2 X^2(0)} . \quad (4)$$

The function $[\kappa(z)-1]/z$ is analytic in the complex plane cut from 0 to 1 along the real axis. A direct application of Cauchy's theorem around this cut yields

$$\frac{\kappa(z)-1}{z} = \frac{1}{2\pi i} \int_0^1 \frac{[\kappa^+(\mu)-\kappa^-(\mu)]d\mu}{\mu(\mu-z)} . \quad (5)$$

The boundary values of $\kappa(z)$ as given by Eq. (4) are inserted into the integrand of Eq. (5). After some rearrangement, we obtain the nonlinear integral equation

$$\kappa(-z) = 1 - z \int_0^1 \frac{[1-\mu^2 X^2(0)]f(\mu)d\mu}{(1-\mu^2/\eta_1^2)(\mu+z)\kappa(-\mu)} . \quad (6)$$

This is a nonlinear singular integral equation because from Eq. (2)

$|f(\mu)| \rightarrow \infty$ as $\mu \rightarrow 1/\sigma$. By defining

$$g(\mu, z) = \frac{[1-\mu^2 X^2(0)]\mu}{\left(1 - \frac{\mu^2}{\eta_1^2}\right)(\mu+z)\kappa(-\mu)} \quad (7)$$

and by the standard technique of subtracting the singularity,⁴ Eq. (6) becomes

$$\begin{aligned}
\kappa(-z) = & 1 - z \int_0^1 \frac{g(\mu, z)}{\mu} \{C_{22} + [C_{11} - 2C\mu\tau(\mu)]\theta_1(\mu)\}d\mu + 2Cz \int_0^1 [g(\mu, z) \\
& - g(1/\sigma, z)] [\tau(\sigma\mu)\theta_1(\mu) + \tau(1/\sigma\mu)\theta_2(\mu)]d\mu + \frac{2Cz}{\sigma} g(1/\sigma, z) \\
& \times [\sigma\tau(1/\sigma) + \frac{1}{2} \ln(\sigma^2 - 1)]
\end{aligned} \tag{8}$$

where the last term in brackets is obtained by integrating

$$\sigma \int_0^1 [\tau(\sigma\mu)\theta_1(\mu) + \tau(1/\sigma\mu)\theta_2(\mu)]d\mu$$

and Eq. (2) has been used for $f(\mu)$.

Eight point Gauss quadrature is now used in each of the integration intervals $\mu \in [0, 1/\sigma]$ and $\mu \in [1/\sigma, 1]$. An iteration procedure is used to solve Eq. (8) where for the first iteration $\kappa(-z) = 1$. In a sample problem the maximum difference in κ between the fourth and fifth iterations was found to be less than 10^{-6} .

With $\kappa(-z)$ known, the X-function is obtained from Eq. (3). To compute $\gamma(\mu)$, first recall that [Eq. (I-35)]

$$\gamma(\mu) = \frac{\mu X^+(\mu)}{\Omega^+(\mu)}. \tag{9}$$

Then from Eqs. (1b) and (3), we obtain

$$\gamma(\mu) = \frac{\mu\eta_1^2 \left(\frac{1}{X(0)} + \mu \right) X^2(0)}{(\eta_1^2 - \mu^2)\kappa(-\mu)}. \tag{10}$$

With $\gamma(\mu)$ known, we are ready to solve the equations for the expansion coefficients. But first we discuss a fast, accurate method to evaluate singular integrals.

III. NUMERICAL PROCEDURES FOR SINGULAR INTEGRALS AND ITERATION TECHNIQUE

An inspection of the equations that must be solved for the expansion coefficients [Eqs. (I-58)] reveals the fact that the integrands of Cauchy principal value integrals as well as of ordinary integrals contain $\gamma(\mu)$ and logarithmic functions. The computations of numerical values for functions of this type take a relative long time on the computer. Therefore, we use an integration scheme where these functions are computed once and then stored in the fast access memory to be recalled as needed. Specifically, we use the midpoint approximation and trapezoidal rule to evaluate all integrals.

The operator $O(\mu)$ as given by Eq. (I-39) is defined in part by the boundary values of $\Omega(z)$. These boundary values change at $\mu = 1/\sigma$ requiring that we define an independent mesh interval for each of $\mu \in [0, 1/\sigma]$ and $\mu \in [1/\sigma, 1]$ even though the integrands are well-behaved at $\mu = 1/\sigma$. In addition the operator $O(\mu)$ requires the evaluation of singular integrals of the general type

$$P \int_0^1 \frac{F(\mu') d\mu'}{\mu' - \mu}$$

where $F(\mu)$ is ordinarily a product of $\gamma(\mu)$ and logarithmic factors. By usual procedures⁴ the singularity is subtracted to yield

$$P \int_0^1 \frac{F(\mu') d\mu'}{\mu' - \mu} = \int_0^1 \frac{[F(\mu') - F(\mu)] d\mu'}{\mu' - \mu} + F(\mu) \ln \left(\frac{1-\mu}{\mu} \right). \quad (11)$$

For illustrative purposes, assume the singularity is at $\mu = \mu_1$. Then we approximate the principal value integral by

$$P \int_0^1 \frac{F(\mu') d\mu'}{\mu' - \mu} \cong \sum_{j=1}^D \frac{[F(\mu_j) - F(\mu_1)] h_j}{\mu_j - \mu_1} + h_1 F'(\mu_1) + F(\mu_1) \ln \left(\frac{1-\mu_1}{\mu_1} \right). \quad (12)$$

The prime on the summation symbol denotes that the term $j = i$ is not included. This term is given by the second term on the right-hand side of Eq. (12). h_j is the width of interval j and D is the total number of intervals.

When the singular point μ_i is not at the midpoint of the first or last interval or at the midpoint of the intervals adjacent to $\mu = 1/\sigma$ then the second term on the right-hand side of Eq. (12) is approximated by

$$h_i F'(\mu_i) \simeq \frac{1}{2} [F(\mu_{i+1}) - F(\mu_i)] . \quad (13a)$$

Otherwise, we use⁵

$$h_i F'(\mu_i) \simeq \begin{cases} \frac{1}{3} [F(\mu_2) + 3F(\mu_1) - 4F(0)], & i = 1 & (13b) \\ \frac{1}{3} [4F(1/\sigma) - 3F(\mu_P) - F(\mu_{P-1})], & i = P & (13c) \\ \frac{1}{3} [F(\mu_{P+2}) + 3F(\mu_{P+1}) - 4F(1/\sigma)], & i = P+1 & (13d) \\ \frac{1}{3} [4F(1) - 3F(\mu_D) - F(\mu_{D-1})], & i = D & (13e) \end{cases} .$$

Here we denote by the symbol P the total number of intervals for $\mu \in [0, 1/\sigma]$.

Recall that D is the total number of intervals for $\mu \in [0, 1]$.

The midpoint approximation is required in this analysis because we observe that at $\mu = 0$ or $\mu = 1$ the last term in Eq. (11) is singular. These singularities cause no difficulty in the actual analysis because they are removed by the factors multiplying the Cauchy integrals or $F(\mu)$. What we are saying is that the product of the last term of Eq. (11) with $l_1(\mu)^1$ is well-behaved near $\mu = 1$ and $F(\mu) \rightarrow 0$ as $\mu \rightarrow 0$.

The iteration procedure for determining the expansion coefficients will be described with reference to Eqs. (I-58a) and (I-58b). The discrete mode expansion coefficient is approximated as

$$A_+^{(0)} = \frac{\int_0^1 \gamma(\mu) \psi'(\mu) d\mu}{-\eta_1 X(\eta_1) - c \int_0^1 \frac{\gamma(\mu) k(\eta_1, \mu) d\mu}{\eta_1 - \mu}} . \quad (14)$$

With this result substituted into Eq. (I-58b), we obtain

$$\alpha_2^{(1)}(\mu) = o(\mu) \psi'(\mu) - A_+^{(0)} \left\{ \frac{\ell_1(\mu) \eta_1 X(\eta_1)}{\eta_1 - \mu} - c o(\mu) \left[\frac{\eta_1 k(\eta_1, \mu)}{\eta_1 - \mu} \right] \right\} . \quad (15)$$

The superscript on A_+ and $\alpha_2(\mu)$ denotes the iteration index. This value for $\alpha_2(\mu)$ when substituted in Eq. (I-58a) and the double integration performed provides an improved value for A_+ which we denote by $A_+^{(1)}$. Then a new value of $\alpha_2^{(2)}(\mu)$ is computed from Eq. (I-58b),

$$\begin{aligned} \alpha_2^{(2)}(\mu) &= o(\mu) \psi'(\mu) - A_+^{(1)} \left\{ \frac{\ell_1(\mu) \eta_1 X(\eta_1)}{\eta_1 - \mu} - c o(\mu) \left[\frac{\eta_1 k(\eta_1, \mu)}{\eta_1 - \mu} \right] \right\} \\ &+ c o(\mu) \int_0^1 \frac{\eta \alpha_2^{(1)}(\eta) k(\eta, \mu) d\eta}{\eta - \mu} . \end{aligned} \quad (16)$$

Continuing in this manner, the nth iterative solution is obtained as

$$\begin{aligned} \alpha_2^{(n)}(\mu) &= o(\mu) \psi'(\mu) - A_+^{(n-1)} \left\{ \frac{\ell_1(\mu) \eta_1 X(\eta_1)}{\eta_1 - \mu} - c o(\mu) \left[\frac{\eta_1 k(\eta_1, \mu)}{\eta_1 - \mu} \right] \right\} \\ &+ c o(\mu) \int_0^1 \frac{\eta \alpha_2^{(n-1)}(\eta) k(\eta, \mu) d\eta}{\eta - \mu} . \end{aligned} \quad (17)$$

We assume that for physically interesting problems (e.g., Milne and constant source), this procedure converges in the sense that given an $\epsilon > 0$ we can find an integer M such that for all $m > M$ and $\mu \in [0, 1]$,

$$|\alpha_2^m(\mu) - \alpha_2^{(m-1)}(\mu)| < \epsilon .$$

Convergence was achieved in seven iterations for $\epsilon = 10^{-7}$ in the problems studied in this paper. With A_+ and $\alpha_2(\mu)$ known, $\alpha_1(\mu)$ is computed from Eq. (I-58c) thus determining all expansion coefficients.

The expansion coefficients are now substituted into the appropriate equations of I to determine the angular fluxes, total fluxes, and currents for each group.

IV. SPHERICAL HARMONIC SOLUTIONS

The spherical harmonic solutions to Eq. (1) of I in the P_1 , P_3 , and so-called double P_1 (DP_1) approximation are straightforward extensions of the methods developed in the one-group case.⁴ As usual in the P_1 and P_3 approximation the rigorous boundary condition at the vacuum-medium interface is approximated by the Marshak boundary condition while in the DP_1 approximation the exact boundary condition is used. In each approximation method a secular determinant is derived from which the eigenvalues (roots) are obtained. The extrapolation distances for these approximations is defined in a manner consistent with the exact methods of I. Complete details of the spherical harmonic solutions are given in Ref. 6.

V. NUMERICAL RESULTS

For illustrative purposes, we have selected for detailed study four problems in light water media. The first problem which is denoted by Set I is ordinary light water. Set II, III, and IV consist of borated light water at concentrations of 1.025, 2.99, and 6.35 barns/hydrogen atom, respectively.

The ranges of the energy groups are

$$\text{Group 1: } 0 < E < .0253 \text{ eV}$$

and

$$\text{Group 2: } .0253 < E < .532 \text{ eV.}$$

The thermal spectra and cross-section averaging routine were performed by using the INCITE⁷ code. The McMurry-Russell⁸ kernel was used at room temperature (293°K). We list in Table I the results of these cross-section calculations. Recall that the cross sections must be modified to

$$\sigma = \sigma_1/\sigma_2 \quad \text{and} \quad C_{ij} = \sigma_{ij}/2\sigma_2 .$$

From the dispersion equation [Eq. (I-10)], and the secular determinants of the approximation methods, the respective eigenvalues are computed. These eigenvalues are given in Table II. The discrete eigenvalues provide the asymptotic solution in each case. We note that in the low absorption cases (Set I and II) the P_1 discrete eigenvalues are closer to the exact values than the P_3 or PD_1 . As the absorption is increased (Set III and IV) the P_3 and DP_1 approximation provide the more nearly correct discrete eigenvalues. We observe that the DP_1 discrete eigenvalues are in every case nearly identical to the P_3 values. The P_1 approximation in two-group theory yields an eigenvalue in the continuum while in the one-group case only the discrete eigenvalue (asymptotic solution) is calculated.⁴

The expansion coefficients for the exact calculation were calculated for each problem set by the iteration procedure described in Section III. The

shapes of these expansion coefficients for Set I and IV are shown in Fig. 1 and Fig. 2. The expansion coefficients $\alpha_1(\mu)$ and $\alpha_2(\mu)$ are quite smooth and well-behaved except for $\alpha_2(\mu)$ in the range $1/\sigma < \mu < 1$. We observe in every case a resonance-like behavior with the "resonance" becoming higher, more peaked and shifting nearer to $1/\sigma$ as absorption is increased. These are the quasi-discrete modes discussed in Section I.

The calculated extrapolation distances are shown in Table III. The P_1 results in Table III are consistently too low while the P_3 results are too high and with increased absorption the P_1 and P_3 extrapolation distance become progressively less accurate. The DP_1 values are about 3% higher than the P_3 . For the problems studied in this work, the extrapolation distances are the same for each group.

The angular distribution for Group 1, Set I, and constant isotropic source is shown in Fig. 3. The P_1 results appear to give a better fit to the exact results than the P_3 except for the inward contribution. Both the positive and negative inward angular distributions are larger for the P_1 case than for the P_3 . Of course, the exact and DP_1 results give no inward contribution. Also, we note that the DP_1 results for the exit distribution are very close to the exact calculation. Similar results were obtained for Group 2.

The modification in the exact angular distribution for Group 2, Set I with distance in mean free path (m.f.p.) is shown in Fig. 4. We note how the distributions become progressively more nearly isotropic and increase in magnitude with distance into the medium.

The effect of increased absorption on the exit angular distribution for Group 2 is shown in Fig. 5. As a measure of the peaking in the exit distribution we compute the ratio of the angular flux at $\mu = -1$ to that at $\mu = 0$.

This ratio is 2.48 for Set I (pure water) while for Set IV (most poisoned case) it is 2.10. Thus in the constant source problems with increased absorption the peaking becomes less pronounced in the forward (exist) direction. The opposite effect was observed in the Milne problems. Specifically, the ratios for the comparable Milne problems were 2.91 and 3.77 for Set I and Set IV, respectively. These results for the Milne problems are in agreement with one-group theory.⁴

In reactor physics design the total fluxes and currents are of most interest and utility. In Fig. 6 we show the total flux for Group 2, Set IV. On the scale of that figure it is impossible to distinguish the DP₁ results from the exact. The horizontal line gives the asymptotic flux (flux as $z \rightarrow \infty$) for the constant source problem.

In Table IV and V are shown the total fluxes for Group 1, Set I and Group 1, Set IV, respectively. The error is computed by

$$\text{error} = \frac{[\rho_0(\text{approx}) - \rho_0(\text{exact})] \times 100}{\rho_0(\text{exact})} .$$

The P₃ total fluxes are within 1 or 2% of the exact values except at the interface. We note that both the P₁ and P₃ give a negative error except at the interface where the error is several percent positive. The DP₁ calculation yields a significant improvement over the P₃ especially at the interface.

Finally in Fig. 7 the constant source current for Group 2, Set IV is shown. Only the P₁ results departed from the exact results sufficient to show on the figure. Nevertheless, the DP₁ results were nearer the exact results in every case.

VI. CONCLUSIONS

In the general two-group neutron transport problem an exact analytical solution has not been found. Nevertheless, by the Case approach⁴ we have succeeded in deriving a pair of coupled equations which are conveniently solved by numerical methods. One of these equations is a singular integral equation. It may be generally true that singular integral equations are easier to solve than Fredholm equations. At least this work demonstrates that by appropriate numerical analysis and computer programming any real difficulties can be surmounted.

In connection with this work several computer codes were developed in the Michigan Algorithm Decoder Language (MAD) from which any one can (with different cross section sets) test the accuracy of various approximation methods. A complete listing of these codes is given in Ref. 6.

The numerical calculation show that although the P_1 approximation yields fairly good results for the total flux and current the angular distribution is not so well represented especially at the interface and in the inward direction. The P_3 approximation improves on the P_1 in that the inward angular distribution is nearer the exact. The DP_1 improves on both the P_1 and P_3 approximation in angular fluxes, total fluxes and currents. Of course, in the DP_1 approximation we can specify the exact boundary condition. Therefore, we would expect the exit angular distribution to be well represented.

An interesting observation from this study is that in the constant source case the exit angular distribution becomes less pronounced with increased absorption in the medium. We can contrast this with the Milne problem where

the opposite effect is noted. We leave it to the reader to devise a physical explanation for these two effects.

We recall that the P_3 and DP_1 approximations present the same computational difficulty. From this study we conclude that in two-group reactor design analysis (with reactor parameters similar to those used here) the DP_1 approximation gives significantly better results than the P_3 . A similar conclusion is stated by Weinberg and Wigner⁹ in the one-group case but never (to our knowledge) has it been tested against exact calculations in two-group problems.

The most interesting results, however, appear to be the quasi-discrete modes, shown in Figs. 1 and 2, and discussed in more detail in Section I.

VII. ACKNOWLEDGMENTS

One of the authors (P.F.Z.) wishes to acknowledge with gratitude discussions with Professor G. C. Summerfield. In addition, we wish to thank R. L. Curtis and R. A. Grimesey for providing cross-section data prior to publication.

REFERENCES FOR PART II

1. D. R. Metcalf and P. F. Zweifel, "Solution of the Two-Group Neutron Transport Equation, Part I." Nucl. Sci. Eng., [Equations in this paper will be referred to by Eq. (I-n).]
2. B. Carnahan, H. A. Luther, and J. O. Wilkes, Preliminary Edition of Applied Numerical Methods, John Wiley and Sons, Inc., New York, (1964).
3. F. C. Shure and M. Natelson, Ann. Phys., 26, 274 (1964).
4. K. M. Case and P. F. Zweifel, Linear Transport Theory, Addison-Wesley Publishing Company, Reading, Massachusetts (1967).
5. E. H. Bareiss and C. P. Neumann, "Singular Intergrals and Singular Integral Equations with a Cauchy Kernel and the Method of Symmetric Pairing," ANL 6988, Argonne National Laboratory (1965).
6. D. R. Metcalf, Thesis, The University of Michigan (1968).
7. R. L. Curtis and R. A. Grimesey, "INCITE - A Fortran IV Program to Generate Neutron Spectra and Multigroup Constants Using Arbitrary Scattering Kernels," IN-1062, Idaho Nuclear Corporation (to be published).
8. H. L. McMurry, G. J. Russell and R. M. Brugger, Nucl. Sci. Eng., 25, 248 (1966).
9. A. M. Weinberg and E. P. Wigner, The Physical Theory of Neutron Chain Reactors, University of Chicago Press, Chicago (1958).

TABLE I

TWO-GROUP MACROSCOPIC CROSS SECTIONS

Set No.	σ_1	σ_2	σ_{1a}	σ_{2a}	σ_{11}	σ_{22}	σ_{12}	σ_{21}
I	4.8822	3.2343	.03166	.01498	3.8180	2.8669	.3524	1.0326
II	4.9270	3.1686	.09725	.04424	3.7953	2.8005	.3239	1.0345
III	5.0914	3.0707	.28011	.11738	3.7659	2.6828	.2705	1.0454
IV	5.3220	2.9738	.58336	.22326	3.6906	2.5341	.2164	1.0481

TABLE II
EIGENVALUES OF THE TWO-GROUP NEUTRON TRANSPORT EQUATION

Set No.	Exact		P ₁		P ₃		DP ₁	
	Discrete	Continuum	Discrete	Continuum	Discrete	Continuum	Discrete	Continuum
I	7.1869	0 < η < 1	7.2482	.7435	7.2647	.8599	7.2636	.8359
					.4835		.2786	
					.3040		.1760	
II	4.1793	0 < η < 1	4.1746	.7158	4.2040	.8293	4.2019	.8054
					.4823		.2780	
					.2941		.1703	
III	2.5958	0 < η < 1	2.5456	.6494	2.5961	.7569	2.5918	.7333
					.4788		.2765	
					.2725		.1581	
IV	1.9361	0 < η < 1	1.8638	.5683	1.9363	.6704	1.9278	.6466
					.4730		.2740	
					.2479		.1444	

TABLE III

EXTRAPOLATION DISTANCES FOR MILNE PROBLEMS

Set No.	Exact	P_1	P_3	DP_1
I	.6658	.6217	.6736	.6944
II	.6783	.6286	.7111	.7320
III	.7121	.6476	.7976	.8177
IV	.7613	.6735	.9279	.9432

TABLE IV

TOTAL FLUXES FOR GROUP 1, SET I, CONSTANT SOURCE

Distance (m.f.p.)	Exact	PM	Error	P_3	Error	DP_1	Error
0	1.4106	1.5966	+13.1	1.4631	+3.7	1.3975	-.9
.5	3.4424	3.3089	- 3.9	3.3768	-1.9	3.43649	-.2
1.0	5.0450	4.8649	- 3.6	4.9675	-1.5	5.0164	-.6
1.5	6.4926	6.2946	- 3.0	6.4008	-1.4	6.4449	-.7
2.0	7.8245	7.6194	- 2.6	7.72079	-1.3	7.7613	-.8
3.0	10.2009	9.9946	- 2.0	10.0829	-1.2	10.1198	-.8
5.0	14.0417	13.8530	- 1.3	13.9153	- .8	13.9427	-.8
10.0	20.0287	19.8987	- .6	19.9292	- .5	19.9362	-.5

TABLE V

TOTAL FLUXES FOR GROUP.1, SET IV, CONSTANT SOURCE

Distance (m.f.p.)	Exact	P ₁	Error	P ₃	Error	DP ₁	Error
0	3.2683	3.6563	+11.8	3.4227	+4.6	3.2625	-.2
.5	8.3076	7.9138	- 4.7	8.2312	- .9	8.3723	+ .8
1.0	11.5025	11.1189	- 3.3	11.4584	- .4	11.5392	+ .3
1.5	13.8524	13.5497	- 2.2	13.8201	- .2	13.8656	+ .1
2.0	15.6174	15.3999	- 1.4	15.5924	- .2	15.6174	- 0
3.0	17.9790	17.8879	- .5	17.9585	- .1	17.9702	0
5.0	20.1820	20.1908	+ 0	20.1717	- .1	20.1776	0
10.0	21.2945	21.3033	+ 0	21.2945	+ 0	21.2959	0

FIGURE CAPTIONS

Fig. 1. Expansion coefficients for Milne problem, Set I.

Fig. 2. Expansion coefficients for Milne problem, Set IV.

Fig. 3. Constant source angular distribution for Group 1, $\psi_1(0, \theta)$.

Fig. 4. Modifications in exact angular distribution with distance into the medium, Set I, Group 2.

Fig. 5. Absorption effect on exact angular distribution for constant source problem, Set I and IV, Group 2.

Fig. 6. Total flux for the constant source vs. distance into the medium, Set IV, Group 2.

Fig. 7. Constant source current vs. distance for Group 2, Set IV.

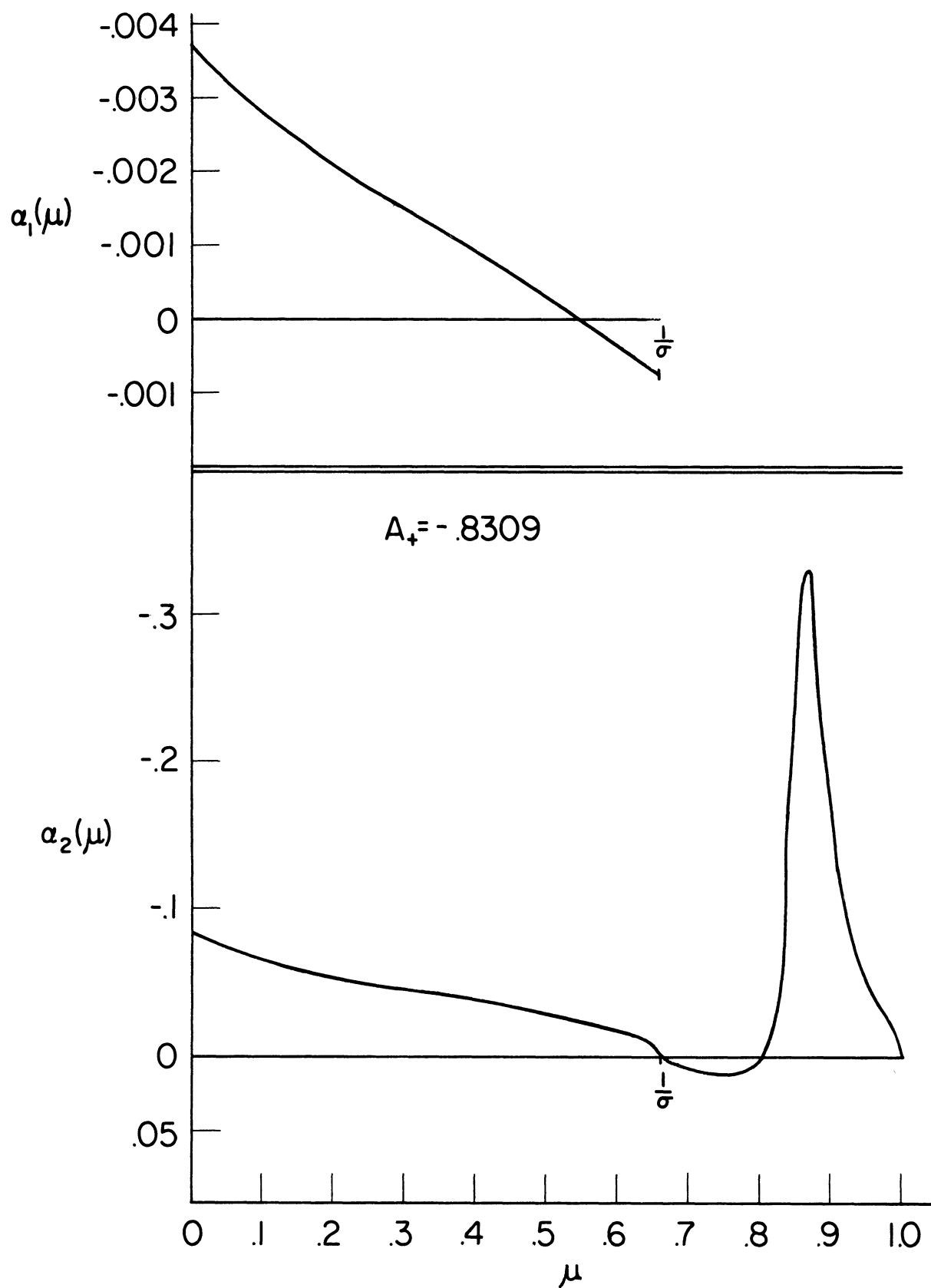


Fig. 1.

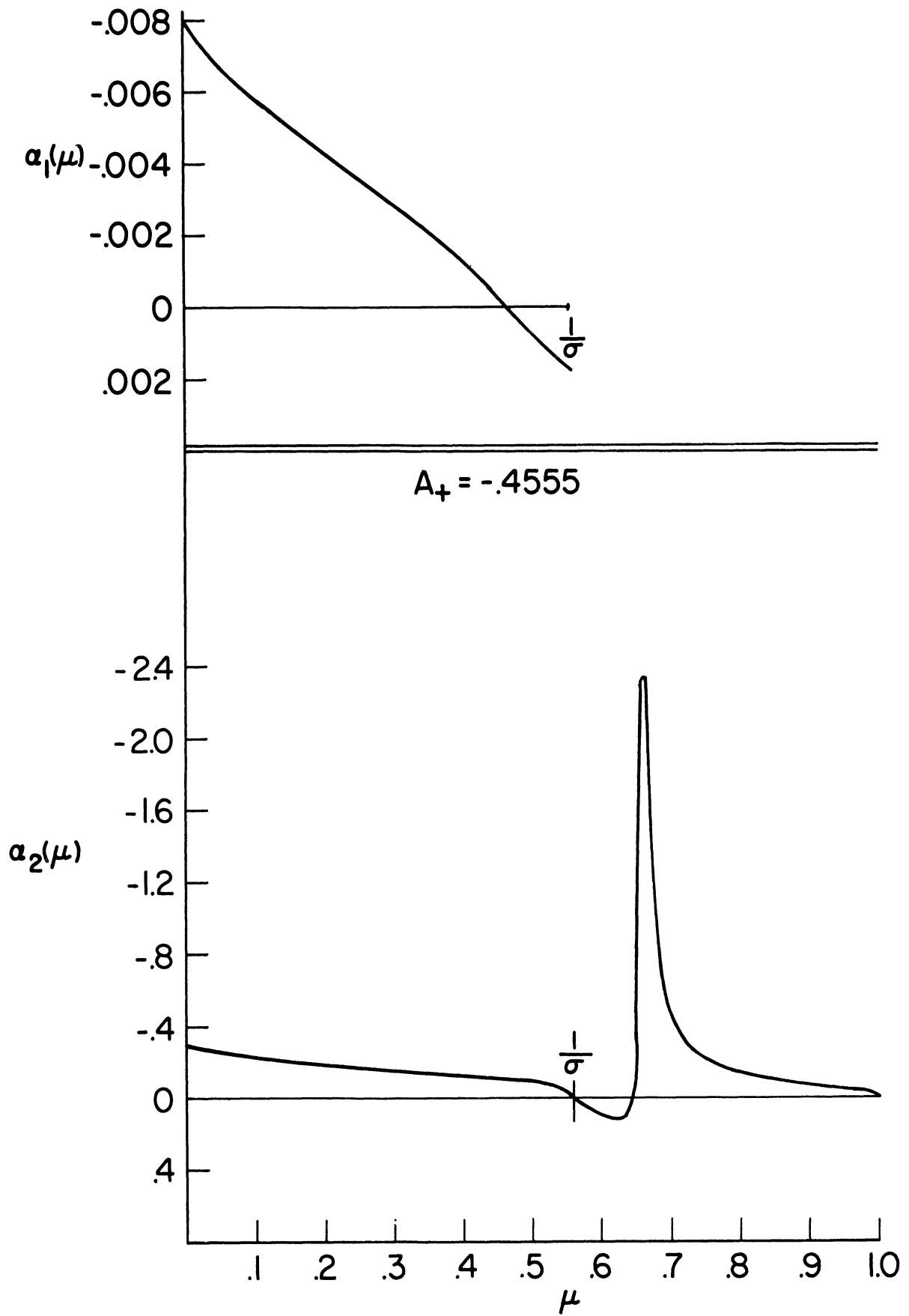


Fig. 2.

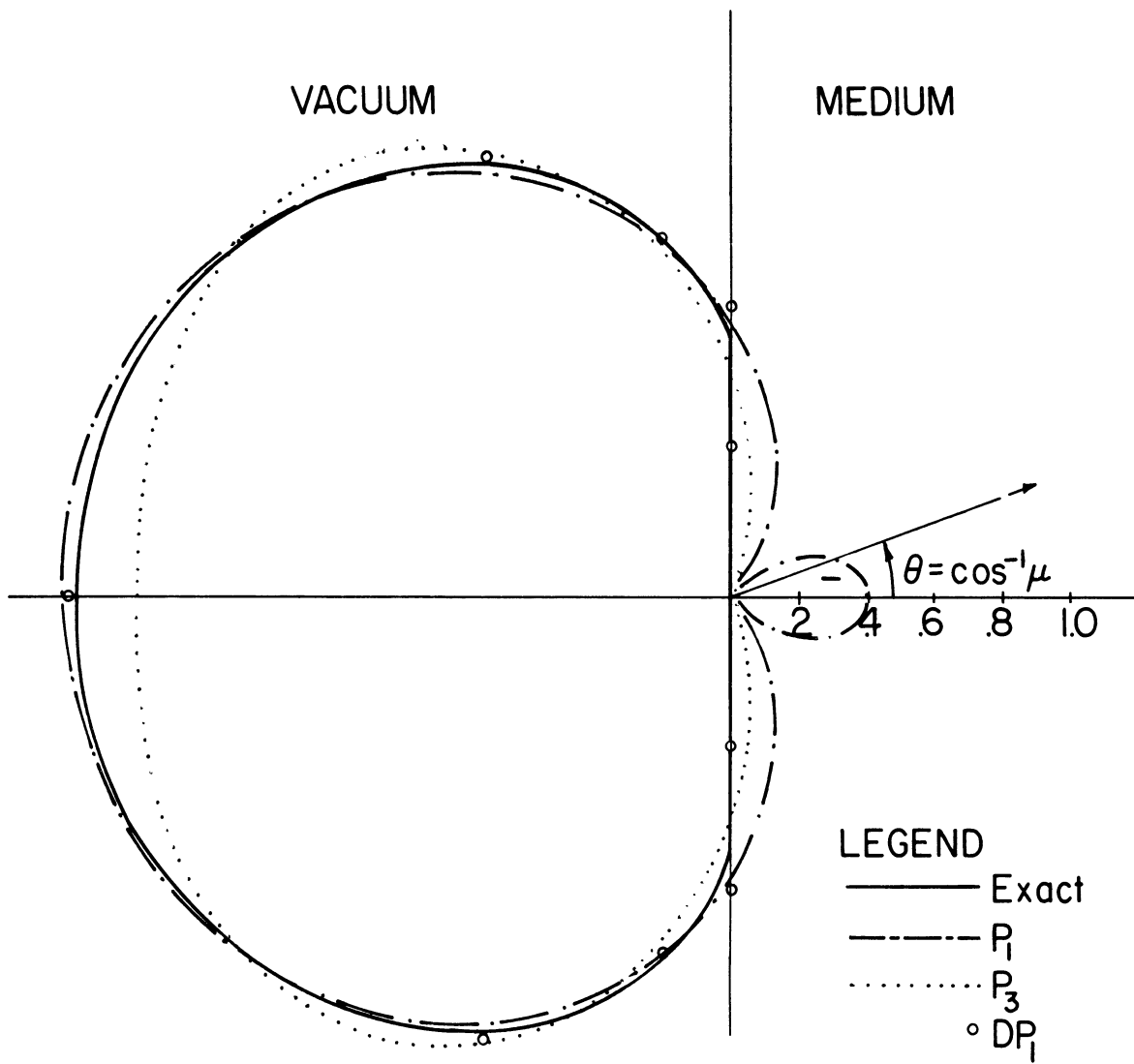


Fig. 3.

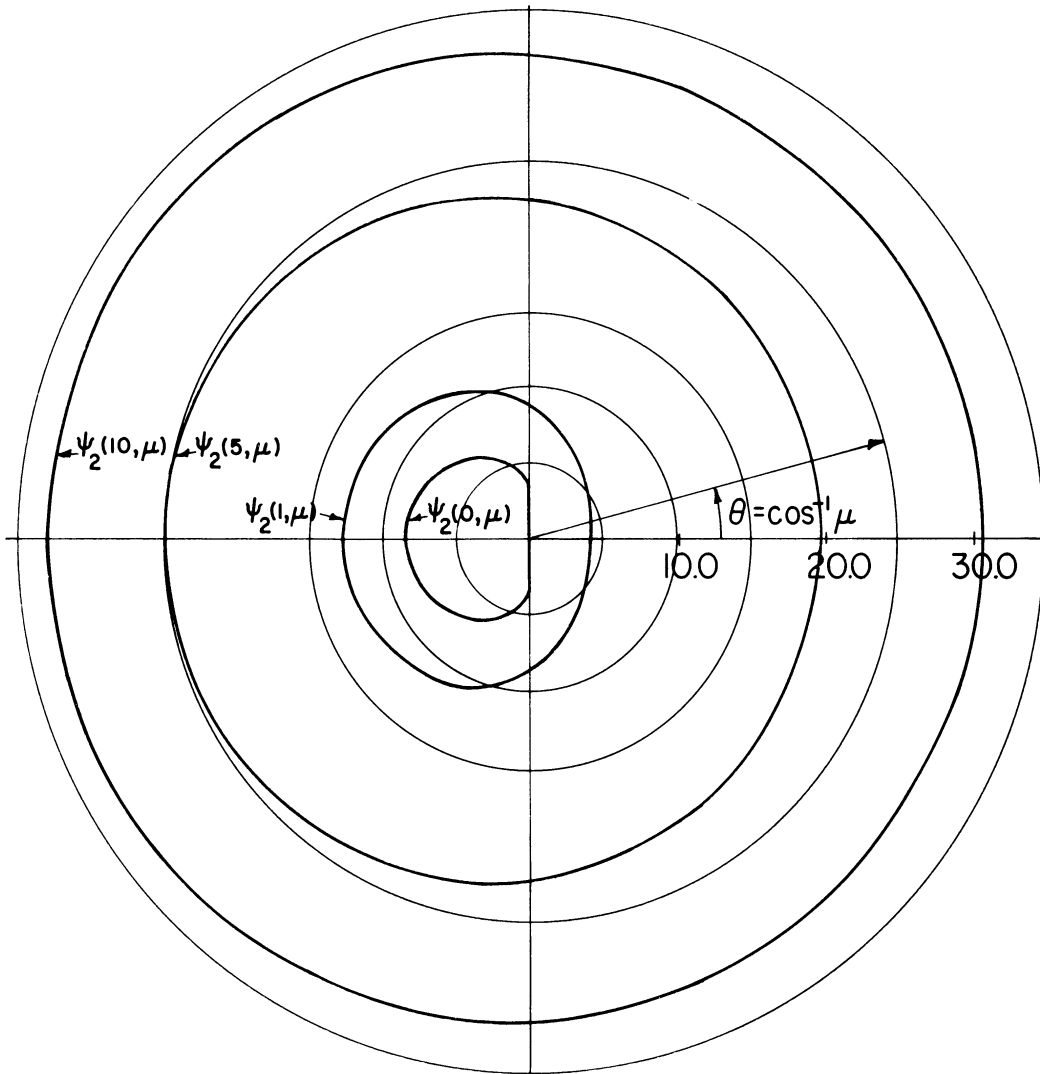


Fig. 4.

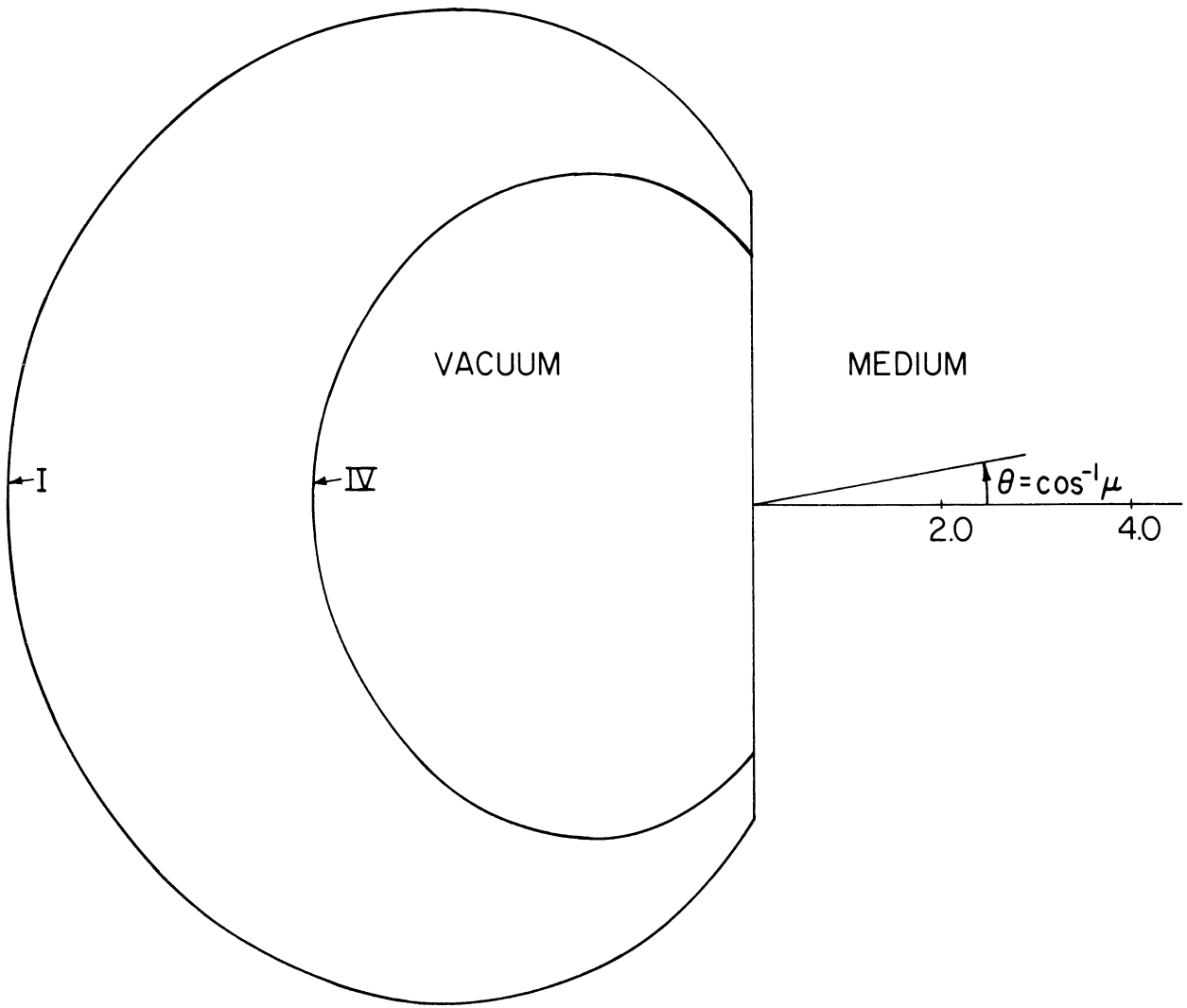


Fig. 5.

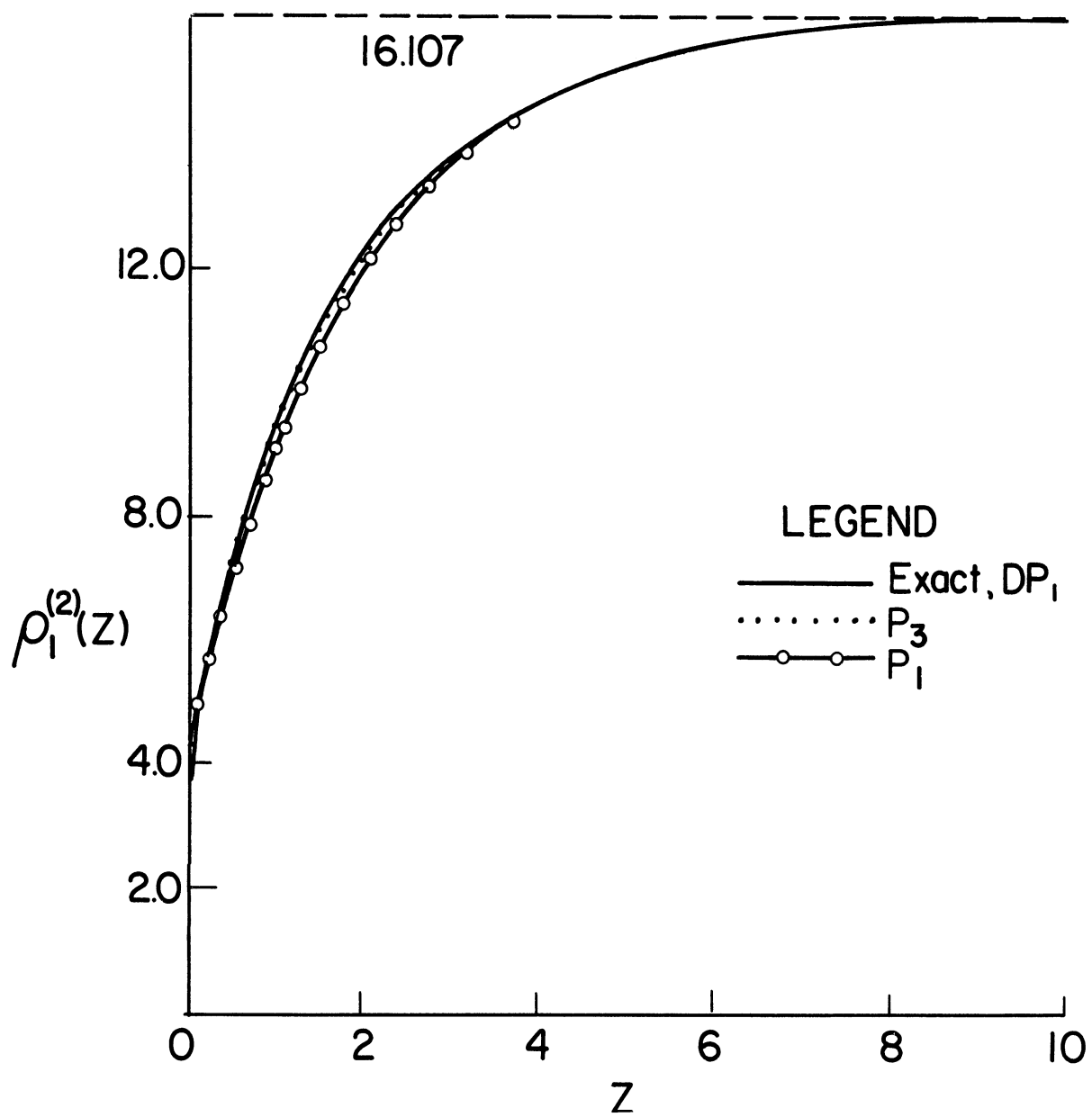


Fig. 6.

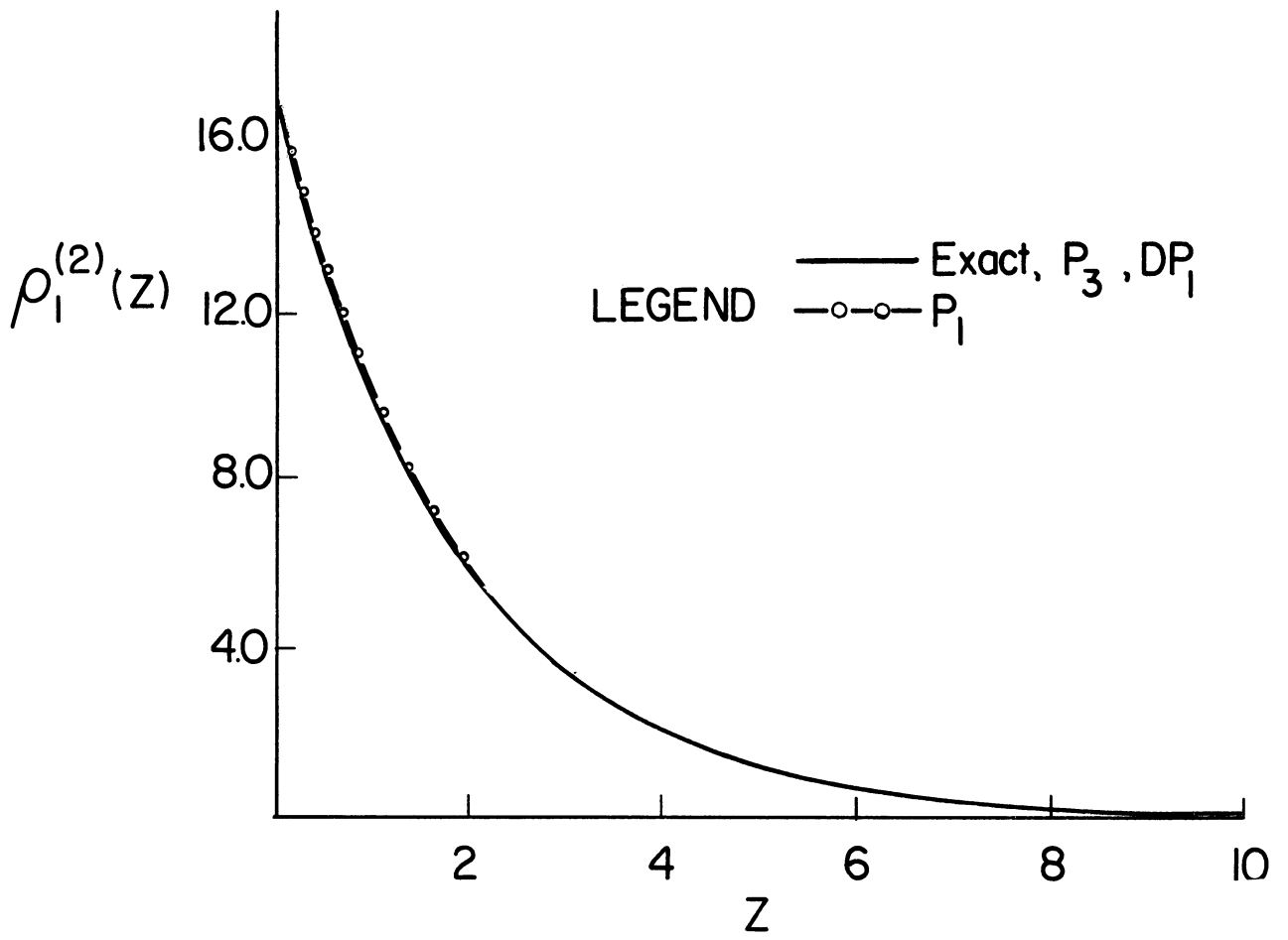


Fig. 7.

